Molecular Biology of the Cell
Vol. 16, 2382–2394, May 2005

Vertebrate Nup53 Interacts with the Nuclear Lamina and Is Required for the Assembly of a Nup93-containing Complex[D]

Lisa A. Hawryluk-Gara, Ellen K. Shibuya, and Richard W. Wozniak

Department of Cell Biology, University of Alberta, Edmonton, Alberta, Canada T6G 2H7

Submitted October 1, 2004; Revised January 31, 2005; Accepted February 2, 2005
Monitoring Editor: Karsten Weis

The nuclear pore complex (NPC) is an evolutionarily conserved structure that mediates exchange of macromolecules across the nuclear envelope (NE). It is comprised of ~30 proteins termed nucleoporins that are each present in multiple copies. We have investigated the function of the human nucleoporin Nup53, the ortholog of *Saccharomyces cerevisiae* Nup53p. Both cell fractionation and in vitro binding data suggest that Nup53 is tightly associated with the NE membrane and the lamina where it interacts with lamin B. We have also shown that Nup53 is capable of physically interacting with a group of nucleoporins including Nup93, Nup155, and Nup205. Consistent with this observation, depletion of Nup53 using small interfering RNAs causes a decrease in the cellular levels of these nucleoporins as well as the spindle checkpoint protein Mad1, likely due to destabilization of Nup53-containing complexes. The cellular depletion of this group of nucleoporins, induced by depleting either Nup53 or Nup93, severely alters nuclear morphology producing phenotypes similar to that previously observed in cells depleted of lamin A and Mad1. On basis of these data, we propose a model in which Nup53 is positioned near the pore membrane and the lamina where it anchors an NPC subcomplex containing Nup93, Nup155, and Nup205.

INTRODUCTION

The nuclear envelope (NE) is a specialized membrane system that functions to separate the eukaryotic genome from the cytoplasm. The NE consists of an inner and an outer nuclear membrane. The former contains a distinct set of associated proteins, whereas the latter is structurally equivalent to the endoplasmic reticulum (reviewed in Mattaj, 2004). The nucleoplasmic face of the metazoan inner nuclear membrane is connected to a fibrous protein meshwork termed the nuclear lamina that forms a shell around the underlying chromatin mass. The lamina is composed of A- and B-type lamins, which are closely related to one another and to the intermediate filament-like family of proteins (reviewed in Burke, 2001). The nuclear lamina has been suggested to be involved in maintaining the structural integrity of the NE and influencing chromatin structure and function. The association of the lamina with transcriptionally inactive heterochromatin has led to the suggestion that it may play a role in regulating gene expression and some recent data support this idea (reviewed in Mattout-Drubezki and Gruenbaum, 2003).

At numerous points along the NE the inner and outer nuclear membranes fuse to form pores ~100 nm in diameter. These pores are occupied by complex macromolecular structures termed nuclear pore complexes (NPCs). The NPCs are associated with euchromatin channels that extend into the interior of the nucleus, interrupting the continuity of the lamina and the heterochromatin. These complex structures have an estimated mass of ~60 million Daltons, but are composed of a relatively small number of proteins (~30; Rout *et al.*, 2000; Cronshaw *et al.*, 2002) termed nucleoporins or nups. This is explained by the fact that all of these proteins appear to be present in multiple copies within the NPC, with groups of nups forming the repetitive subcomplexes that give the NPC its characteristic eightfold by twofold symmetry (Yang *et al.*, 1998; Rout *et al.*, 2000).

NPCs are believed to regulate all transport into and out of the nucleus. In addition to acting as a diffusion channel for small molecules and metabolites, the NPCs work in conjunction with soluble transport factors to control transport of macromolecules through their central channels. Although the exact mechanism of transport through the NPC has not been clearly defined, some general principles are well accepted. Transport cargos containing nuclear import or export signals are recognized by members of a family of transport factors termed karyopherins, which are capable of functioning in nuclear import (importins) or export (exportins) or in some cases both (Yoshida and Blobel, 2001). The kaps escort their cargos to the NPC, where the kaps bind to members of a family of nups that contain multiple phenylalanine-glycine (FG) repeat motifs within their primary structure. These repetitive peptides directly mediate the binding of the kaps to the FG-nups (reviewed in Ryan and Wente, 2000). Because these nups are located all along the channel through the NPC, most of the current transport models propose that the FG binding sites play an essential role in the movement of the kap/cargo complex through the NPC. Two separate, yet related, models have been proposed to explain this movement. One model suggests that the FG-nups form a hydrophobic network that is selectively

This article was published online ahead of print in *MBC in Press* (http://www.molbiolcell.org/cgi/doi/10.1091/mbc.E04–10–0857) on February 9, 2005.

[D] The online version of this article contains supplemental material at *MBC Online* (http://www.molbiolcell.org).

Address correspondence to: Richard W. Wozniak (rick.wozniak@ualberta.ca).

permeabilized by kaps (Ribbeck and Gorlich, 2001, 2002). Another proposes that the FG-nups are filamentous and form a "virtual gate" by entropically excluding molecules that cannot interact with them (Rout *et al.,* 2000, 2003). By interacting with the FG-nups, kaps overcome this barrier and progress through the channel. Both of these models rely on the idea that the kap-nup interaction is weak (Ribbeck and Gorlich, 2001) or rapidly dissociated (Gilchrist *et al.,* 2002) in order to achieve rates of import sufficient to accommodate the huge flow of molecules across the NE (see Macara, 2001; Weis, 2003 for reviews of transport models).

The apparent modular organization of the NPC observed by ultrastructural analysis is consistent with the concept that distinct subcomplexes of nups interact to form this complex structure. The framework of these subcomplexes, in many cases, likely consists of nonrepeat containing nups on which the FG-nups are positioned to line the NPC channel. Considerable effort has been directed toward identifying subcomplexes of the NPC and examining their role in transport and the assembly of the NPC. One well-studied and conserved subcomplex is termed the Nup84p complex in *S. cerevisiae* and the Nup107–160 complex in vertebrates. The Nup84p complex consists of the nups Nup84p, Nup85p, Nup120p, Nup133p, Nup145-Cp, and Seh1p (Siniossoglou *et al.,* 1996; 2000; Allen *et al.,* 2002; Lutzmann *et al.,* 2002). Mutations in members of the Nup84p complex display a variety of phenotypes including NPC clustering and NE organization defects (Aitchison *et al.,* 1995a; Siniossoglou *et al.,* 1996; 2000; Belgareh and Doye, 1997), suggesting a role for this complex in NPC assembly. Similarly, the vertebrate counterpart, the Nup107–160 complex, comprised of Nup107, Nup160, Nup133, Nup96, Nup85, Sec13, Nup43, Nup37, and Seh1 (Belgareh *et al.,* 2001; Vasu *et al.,* 2001; Harel *et al.,* 2003; Loïodice *et al.,* 2004) is also required for correct NPC assembly (Boehmer *et al.,* 2003; Harel *et al.,* 2003; Walther *et al.,* 2003). Depletion of this complex from *Xenopus* in vitro NE assembly assays results in nuclei with reduced numbers of NPCs (Harel *et al.,* 2003; Walther *et al.,* 2003). These studies suggest that the Nup107–160 complex functions early in postmitotic NPC formation, as it is recruited to the chromatin before the NE membrane (Walther *et al.,* 2003).

A number of other nup subcomplexes have also been identified that contain both nonrepeat and FG-nups. For example, the yeast nonrepeat nup Nic96p has been detected in association with other nonrepeat nups, including Nup188p (Nehrbass *et al.,* 1996; Zabel *et al.,* 1996), and the FG-nups Nsp1p, Nup49p, and Nup57p (Grandi *et al.,* 1995). This complex has been suggested to play a role in both nuclear transport and NPC formation. Similarly, the vertebrate counterpart of Nic96p, Nup93, exists in a complex with Nup188 and Nup205 (the counterpart of yeast Nup192p; Grandi *et al.,* 1997; Miller *et al.,* 2000). Depletion of this complex from *Xenopus* in vitro NE assembly extracts inhibits NPC formation (Grandi *et al.,* 1997). However, experiments in *Caenorhabditis elegans* suggest depletion of Nup93 or Nup205 does not affect pore formation, but does alter the distribution and permeability of NPCs (Galy *et al.,* 2003).

The analysis of the functions of individual NPC subcomplexes is complicated by the observation that certain nups, including for example Nic96p, are detected in association with separate groups of nups suggesting they are part of multiple distinct subcomplexes. One interpretation of these results is that interactions between nups are potentially regulated. This, in fact, appears to be the case for a yeast subcomplex consisting of the nonrepeat nup Nup170p and the FG-nup Nup53p. The interactions between these nups are altered during the cell cycle (Makhnevych *et al.,* 2003). In interphase, Nup53p interacts with Nup170p but is not detected in association with Nic96p. In contrast, during mitosis Nup53p is released from Nup170p and is instead detected bound to Nic96p. A consequence of this rearrangement is the exposure of a binding site on Nup53p for the karyopherin Kap121p. Binding to Nup53p inhibits the translocation of Kap121p and its cargo into the nucleus, thus specifically regulating this pathway during mitosis (Makhnevych *et al.,* 2003). Other examples of regulated changes in nup interactions have also been observed in *Aspergillus nidulans* (De Souza *et al.,* 2004). Here, alterations in the NPC are correlated with phosphorylation of the nups Gle2/Rae1 and Nup98 by the mitotic kinase NIMA. This modification of the NPC allows the nuclear import of cdc2/cyclinB and appears to be required for normal mitotic progression as NIMA mutants show a mislocalization of cdc2/cyclinB and a late G2 arrest (De Souza *et al.,* 2003, 2004).

In this article, we present data examining the function of the mammalian counterpart of yeast Nup53p and its interactions with neighboring nups. We have detected several evolutionarily conserved interactions between Nup53 and Nup93, Nup155, and Nup205. In addition, depletion analysis suggests Nup53, either directly or indirectly, plays a role in the association of the mitotic checkpoint protein Mad1 with the NPC. Our results also suggest Nup53 interacts strongly with the NE membrane and the nuclear lamina and that this nup is required for normal cell growth and nuclear morphology.

MATERIALS AND METHODS

Isolation of Recombinant Proteins and Antibody Production

The open reading frame (ORF) of *Xenopus laevis* Nup53 was inserted into the *Eco*RI site of pGEX-4T-1 (Amersham Biosciences, Baie D'Urfe, Quebec, Canada). An *Escherichia coli* BL21 strain containing pGEX-Nup53 was grown to an OD_{600} = 0.8 and induced with 1 mM IPTG for 4 h at 30°C. GST-Nup53 was purified on glutathione Sepharose 4B beads (Amersham Biosciences) using the manufacturers instructions, in 50 mM Tris HCl pH 7.4, 150 mM NaCl, 1 mM $MgCl_2$, 0.1% Tween 20, 1 mM dithiothreitol (DTT), and Complete Protease inhibitor cocktail (Roche Diagnostics, Laval, Quebec, Canada). *Xenopus* Nup53 was released from the column by incubation with 0.6 units of thrombin (Sigma-Aldrich, Oakville, Ontario, Canada) per 10 μl of beads for 4 h at room temperature. Purified recombinant *Xenopus* Nup53 was used to elicit antibodies in rabbits. The human Nup53 ORF (accession no. AF514993) was amplified with the Expand High-Fidelity PCR system (Roche Diagnostics) using a Human Fetal Kidney cDNA library (BD Biosciences Clontech, San Jose, CA) as a template. The PCR product was inserted into the *Eco*RI site of pGEX-6P-1 (Amersham Biosciences) and used for the GST-pulldown and in vitro binding experiments described below. The human Nup53 cDNA was also directionally inserted into the *Eco*RI (5′) and *Kpn*I (3′) sites of pEGFP-C1 (BD Biosciences Clontech) for the production of stable HeLa S3 cell lines described below. The human Nup93 ORF (accession no. D42085) was amplified by PCR as indicated above from a plasmid containing NUP93 cDNA (clone name ha01471, gene name KIAA0095, Kazusa DNA Research Institute, Chiba, Japan). The NUP93 PCR product was directionally inserted into the *Bam*HI (5′) and *Kpn*I (3′) sites in pGEX-6P-1. Recombinant Nup93 was expressed and purified as described for Nup53 with the exception that Nup93 was released from the beads by cleavage using the PreScission Protease (Amersham Biosciences)

Transfections and Isolation of Stable Lines

HeLa S3 cells were maintained in DMEM (Invitrogen, Berkeley, CA) supplemented with 10% fetal bovine serum, 1% penicillin/streptomycin, and 1% L-glutamine at 37°C and 5% CO_2. Cells were seeded out 24 h before transfection so that they were 30% confluent on the day of transfection. Cells in a 100-mm culture dish were transfected with 0.5 μg of pEGFP-Nup53 using FuGene (Roche Diagnostics) as instructed by the manufacturer. For isolation of stable lines, HeLa cells transfected with pEGFP-Nup53 were seeded into medium containing 800 μg/ml G418 (Sigma-Aldrich) 48 h after transfection. After 3 wk in selection medium, resulting G418-resistant colonies were isolated and screened both by Western blotting of whole cell extracts using mouse monoclonal GFP antibodies (BD Biosciences PharMingen, San Diego,

CA) and by fluorescence microscopy to detect synthesis of the GFP-Nup53 fusion protein.

Rat Liver Nuclei Isolation, Subfractionation, and Extraction

Rat Liver nuclei and nuclear envelopes (NEs) were prepared as previously described (Blobel and Potter, 1966) with modifications (Wozniak *et al.*, 1989). Purified NEs were extracted with 1 M NaCl, 2 M NaCl, 2 M urea, or 7 M urea in buffer containing 20 mM TEA, pH 7.5, 0.1 mM $MgCl_2$, 1 mM DTT, and Complete Protease inhibitor cocktail (Roche Diagnostics) for 15 min at 4°C at a concentration of 100 A_{260} units/ml. (1 A_{260} unit represents the amount of material derived from 1 A_{260} unit of nuclei; $\sim 3 \times 10^6$ nuclei.) The extracted proteins in the supernatant were separated from the pellet by centrifugation at 20,000 × *g* for 30 min at 4°C and precipitated with a final concentration of 10% trichloroacetic acid (TCA). Alternatively, NEs were extracted with 1% Triton X-100 in buffer containing 20 mM TEA, pH 7.5, 0.1 mM $MgCl_2$, 1 mM DTT, and Complete Protease inhibitor cocktail to solubilize the nuclear membrane. Triton X-100–extracted NEs were then recovered in the pellet fraction after centrifugation at 4000 × *g* for 10 min at 4°C. The extracted NE pellets were then reextracted with 0.1, 0.25, 0.5, or 1 M NaCl in the same buffer as above but lacking Triton X-100 at a concentration of 100 A_{260} units/ml. Supernatant and pellet fractions were produced by centrifugation at 20,000 × *g* for 30 min at 4°C, and proteins were analyzed by SDS-PAGE and Western blotting. Finally, preparation of Empigen BB (Calbiochem-Novabiochem, San Diego, CA) extracted NEs was performed as previously described (Cronshaw *et al.*, 2002).

Sucrose gradient sedimentation was performed as described (Fontoura *et al.*, 1999). Briefly, extracted NEs were recovered by centrifugation at 4000 × *g* for 15 min at 4°C and resuspended (1000 A_{260} units/ml) in 1% Triton X-100, 0.025% SDS, and 0.1 mg/ml heparin in 20 mM TEA, pH 7.5, 0.1 mM $MgCl_2$, and Complete Protease inhibitor cocktail. After centrifugation at 15,000 × *g* for 10 min at 4°C, the supernatant was subsequently loaded onto a 10–40% (wt/vol) sucrose gradient containing 20 mM TEA, pH 7.5, 0.1 mM $MgCl_2$, and Complete Protease inhibitor cocktail. Gradients were then centrifuged in a Beckman SW 41 rotor (Fullerton, CA) at 40,000 rpm for 17 h at 4°C. Fractions (750 μl) were collected and precipitated with a final concentration of 10% TCA. Proteins were separated by SDS-PAGE and analyzed by Western blotting.

Isolation of HeLa Cell Extracts

To isolate total HeLa cell extracts, cells were detached from the culture wells by incubating with 0.05% trypsin-EDTA (Invitrogen, Burlington, Ontario, Canada) for 5 min at 37°C. Cells were washed with phosphate-buffered saline (PBS) and counted with a hemocytometer. Cells were then pelleted, solubilized in SDS-PAGE sample buffer at a concentration of 10^5 cells/10 μl of sample buffer, and sonicated for 15 s before incubation at 80°C for 20 min. Proteins from 10 μl of each sample were separated by SDS-PAGE and transferred to nitrocellulose for subsequent Western blotting.

Western Blotting

For the analysis of rat liver NE fractions, proteins were resuspended in SDS-PAGE sample buffer and 1 A_{260} unit per lane analyzed by SDS-PAGE. Nitrocellulose membranes were incubated in 5% skim milk powder in PBS containing 0.1% Tween 20 for 1 h to block nonspecific binding. Antibodies were incubated with the membranes for 1 h at room temperature using rabbit polyclonal antibodies directed against Nup53, gp210 (ImmuQuest, Cleveland, United Kingdom), Nup205 (kindly provided by D. Forbes), Nup93 (BD Biosciences PharMingen, San Diego, CA), lamin B (Chaudhary and Courvalin, 1993), lamin A/C (Chaudhary and Courvalin, 1993), Nup107 (kindly provided by V. Doye), and mouse monoclonal antibodies directed against Nup153 (kindly provided by M. Lohka) and α-tubulin (Sigma-Aldrich). Nup358, Nup214, Nup153, and p62 were detected with mAb414 (BAbCo, Berkeley, CA). Rat antibodies were used to detect Mad1 (kindly provided by T. Yen) and guinea pig antibodies used to detect Nup155 (kindly provided by V. Cordes). Primary antibodies were detected with donkey anti-rabbit, sheep anti-mouse (Amersham Biosciences), goat anti-guinea pig, and goat anti-rat (Sigma-Aldrich) HRP-conjugated secondary antibodies and the ECL system (Amersham Biosciences).

Immunofluorescence

HeLa cells grown on coverslips were washed twice with PBS and then fixed in 3.7% formaldehyde in PBS for 20 min at room temperature. Cells were then permeabilized with 0.2% Triton X-100 in PBS for 5 min at room temperature and subsequently blocked in 2% skim milk powder in PBS-T (PBS containing 0.1% Tween 20) for 2 h. For detection of Nup93, Nup205, and Mad1, cells were preextracted with 0.2% Triton X-100 in PBS before fixation with formaldehyde. Primary antibody incubations were carried out for 1 h at room temperature using rabbit antibodies directed against Nup53 (above), Nup93 (above), emerin (kindly provided by B. Burke), Nup107 (kindly provided by V. Doye), lamin B (Chaudhary and Courvalin, 1993), lamin A/C (Chaudhary and Courvalin, 1993), and guinea pig antibodies directed against Nup155 and Nup 205 (kindly provided by V. Cordes). Nup358, Nup214, Nup153, and p62 were detected with mAb414. For detection of Nup53, antibodies were first affinity purified as described (Harlow and Lane, 1988) with modifications (Marelli *et al.*, 1998). After incubation with primary antibodies, coverslips were washed three times with PBS-T over a period of 45 min. Antibody binding was detected with donkey anti-mouse antibodies conjugated to Cy3 or FITC, donkey anti-rabbit antibodies conjugated to Cy3, or donkey anti-guinea pig antibodies conjugated to Cy3 (Jackson ImmunoResearch Laboratories, West Grove, PA). Nuclear DNA was visualized with the DNA-specific Hoechst No. 33342 Dye (Sigma-Aldrich). Digitonin permeabilization experiments were performed as described (Joseph *et al.*, 2002). Briefly, cells on coverslips were incubated with 0.005% high purity digitonin (Calbiochem-Novabiochem) in transport buffer (110 mM KOAc, 20 mM HEPES, pH 7, pH 7.3, 2 mM $Mg(OAc)_2$, 0.5 mM EGTA, 0.2 mM DTT, and 1 μg/ml each of leupeptin, pepstatin, and aprotinin) for 5 min at room temperature before fixation with 3.7% formaldehyde. All subsequent steps were performed as described for other immunofluorescence experiments with the exception that transport buffer was used instead of PBS-T. For visualization of immunofluorescent images, coverslips were mounted in Vectashield mounting medium (Vector Laboratories, Burlington, Ontario, Canada). All microscopic images were obtained on a Zeiss Axiovert 100M coupled with a Zeiss LSM510 laser scanning system . Images were obtained with a 63 × plan-apochromat objective (Zeiss, Jena, Germany).

GST-pulldown and In Vitro Binding Assays

One hundred A_{260} units of purified rat liver NEs were extracted with a combination of 1% Triton X-100 and 400 mM NaCl in 20 mM Tris pH 7.5, 1 mM DTT, 0.1% Tween 20 and Complete Protease inhibitor cocktail at 4°C for 5 min. Extracted proteins were collected in the supernatant fraction after centrifugation at 20,000 × *g* for 30 min at 4°C. The supernatant was diluted 3.75-fold to a final concentration of 0.3% Triton X-100 and 106 mM NaCl. The diluted rat liver NE fraction (66 A_{260} units/ml) was incubated with 10 μl of glutathione Sepharose 4B beads (Amersham) and preloaded with ~6 μg of GST, GST-Nup93, or GST-Nup53, for 2 h at 4°C. After extensive washing of the beads with 20 mM Tris pH 7.5, 106 mM NaCl, 0.3% Triton X-100, 0.1% Tween 20, 1 mM DTT, and Complete Protease inhibitor cocktail, proteins were eluted from the beads with SDS-PAGE sample buffer and separated by SDS-PAGE. Gels were then silver-stained or transferred to nitrocellulose for Western blotting.

For the in vitro binding assays, ~5 μg of purified, recombinant Nup93 was incubated for 2 h at 4°C with 10 μl of glutathione Sepharose 4B beads preloaded with ~10 μg of GST or GST-Nup53. After washing, proteins were eluted from the beads with SDS-PAGE sample buffer and then separated by SDS-PAGE. Nup93 was detected with either Coomassie Blue or Western blotting.

Mass Spectrometry Identification

Proteins detected by silver staining in the GST-Nup53 pulldown experiment were excised from the SDS-polyacrylamide gel and subjected to in-gel trypsin digestion followed by LC/MS on a CapLC HPLC (Waters, Milford, MA) coupled with a Q-ToF-2 mass spectrometer (Micromass, Manchester, United Kingdom). Subsequent protein identification was performed by searching the nonredundant NCBI database using Mascot Daemon (Matrix Science, London, United Kingdom).

siRNA Methods

Human Nup53 (accession no. AF514993) siRNAs were designed as described (Elbashir *et al.*, 2001). The siRNAs were designed to target 5′-AACCUGCAAGUACUCCUAGGA-3′ of the Nup53 mRNA, corresponding to nucleotides 827–847 relative to the start codon and were synthesized by Qiagen-Xeragon (Germantown, MD). HeLa cells were incubated with 480 nM siRNAs in Oligofectamine (Invitrogen) as described (Harborth *et al.*, 2001). As controls, cells were exposed to either Oligofectamine alone (mock), or an ineffective siRNA duplex (nonsense siRNA) consisting of a scrambled sequence of the Nup53 siRNA.

RT-PCR

The RNeasy RNA-preparation kit (Qiagen, Mississauga, Ontario, Canada) was used to isolate total RNAs from HeLa cells and the reverse transcription reactions were carried out using the OneStep RT-PCR kit (Qiagen). Template RNA (0.5 μg) and gene-specific primers (0.6 μM) were used in a final reaction volume of 50 μl. RT-PCR products were analyzed by agarose gel electrophoresis and ethidium bromide staining.

Cell Cycle Analysis by Fluorescence-activated Cell Sorting

HeLa cells were detached from the culture wells by incubating with 0.05% Trypsin-EDTA for 5 min at 37°C. The cells were subsequently fixed in −20°C 70% ethanol and incubated overnight at 4°C. The fixed cell pellets were washed with PBS and then incubated with 0.1% Triton X-100, 0.2 mg/ml propidium iodide, and 0.2 mg/ml DNase-free RNase A in PBS for 1 h at room temperature. Fluorescence-activated cell sorting (FACS) data were collected

on a FACS Scan (Becton Dickinson, San Jose, CA) and analyzed using CellQuest software.

RESULTS

Characterization of a Vertebrate Counterpart to the Yeast Nucleoporin Nup53p

Amino acid sequence analysis has previously identified potential vertebrate orthologues of the *S. cerevisiae* nucleoporin Nup53p (Marelli *et al.*, 1998). These multiple ORFs encode proteins with molecular masses between 35 and 36 kDa and exhibit similarity to Nup53p in four distinct regions, each separated by an insertion in the larger yeast version (unpublished data). Included in these conserved regions are phenylalanine-glycine (FG) repeat motifs, several potential phosphorylation sites, and a putative C-terminal amphipathic helix (Marelli *et al.*, 2001).

An unspecified vertebrate ORF with similarity to yeast Nup53p has previously been tagged with GFP and, after expression of the fused gene in human HeLa cells, the chimeric protein (termed Nup35-GFP) was localized to the NE in a punctate pattern characteristic of NPC localization (Cronshaw *et al.*, 2002). We have elicited polyclonal antibodies in rabbits directed against a recombinant form of the putative *Xenopus* Nup53 to use as a tool to examine the localization and function of the endogenous form of the vertebrate orthologues. These antibodies react with all vertebrate forms of the protein so far examined, including those derived from human and rat origins (unpublished data). After affinity purification, these antibodies were used to examine the localization of the putative human Nup53 in HeLa cells using immunofluorescence microscopy. The antibody decorated the surface of the NE in a punctate pattern coincident with the position of NPCs, as judged by colocalization with nups recognized by the monoclonal antibody (mAb) mAb414 (Figure 1A). A similar pattern was detected with a GFP-tagged chimera of the human ORF (Figure 1B). In addition, Western blotting analysis was used to evaluate the subcellular fractionation properties of the putative vertebrate Nup53. The results of these experiments demonstrated that the endogenous protein was enriched in fractions of purified rat liver nuclei and NEs (Figure 1C), further supporting its classification as a nup. We propose to designate this protein as Nup53 (in contrast to the previously proposed Nup35). This nomenclature more clearly depicts the relationships between nups of different species and is consistent with that which has been used to name vertebrate nups first identified in yeast (Belgareh *et al.*, 2001).

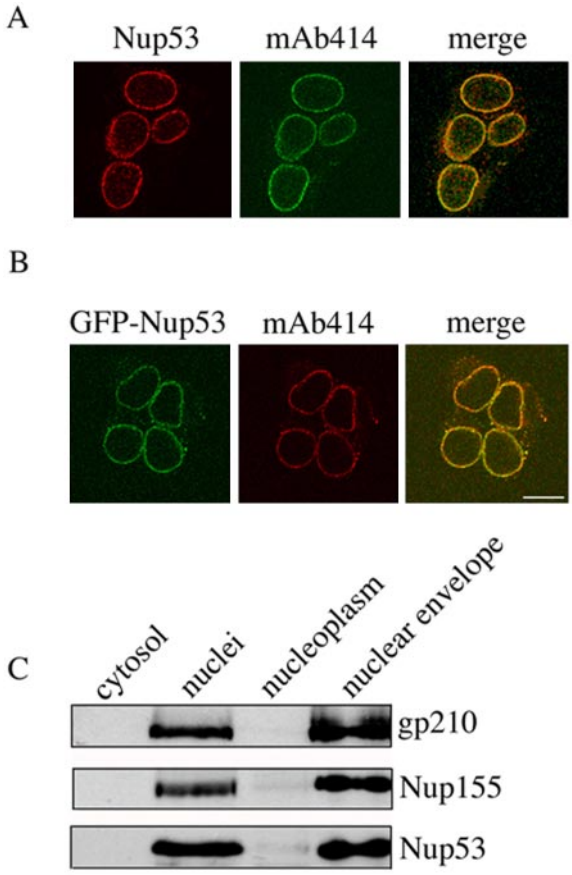

Figure 1. Localization of endogenous Nup53 to the NPC. (A) HeLa cells were processed for immunofluorescence microscopy and probed with affinity-purified rabbit antibodies directed against a putative vertebrate counterpart of Nup53 and a mouse mAb (mAb414) that binds a subset of FG-nups. Binding was detected with Cy3- and FITC-labeled secondary antibodies, respectively. Images of both fluorophores were acquired using a confocal microscope. Merged images are shown on the right. (B) HeLa cells were transfected with a plasmid encoding GFP-Nup53 and a stable cell line was isolated. Cells were fixed and probed with mAb414 as in A but detected with Cy3-labeled secondary antibodies. The cellular distribution of GFP-Nup53 (green), the mAb414 reactive nups (red), and a merged image are shown. Bar, 10 μm. (C) Proteins derived from indicated rat liver subcellular fractions were separated by SDS-PAGE and probed with Nup53-specific antibodies, as well as antibodies directed against the NPC proteins gp210 and Nup155. Nup53 was detected in fractions enriched in nuclei and nuclear envelopes.

Nup53 Is Tightly Associated with the Nuclear Membrane and Lamina

In yeast, Nup53p is part of a defined subcomplex of nups (Marelli *et al.*, 1998; Fahrenkrog *et al.*, 2000; Lusk *et al.*, 2002) and Nup53p has been suggested to interact directly with the NE membrane (Marelli *et al.*, 2001). We have examined the association of vertebrate Nup53 with NEs using differential extraction procedures and Western blotting. For these experiments, isolated rat liver NEs were extracted with salts, detergents, or urea, and the extracted proteins were separated from the membrane and/or insoluble lamina by centrifugation. We have previously used urea extraction procedures to selectively extract nups from the NE membrane and the nuclear lamina (Radu *et al.*, 1993). As shown in Figure 2A, extraction of NEs with 2 M urea quantitatively releases Nup93, Nup153, and Nup155 from a membrane fraction containing the integral protein gp210. In contrast, the majority of Nup53 remains in a pelletable fraction with the lamins (as exemplified by lamin B). The extraction of Nup53 also parallels that of lamins at higher concentrations of urea, where the majority of Nup53 and lamin B were extracted from the NE with 7 M urea (Figure 2A). Similarly, we observed that, although the treatment of NEs with 2 M NaCl partially extracted Nup93, Nup153, and Nup155, Nup53 remained exclusively in the pellet fraction with the lamins.

The most likely explanation for these results is that Nup53 interacts more tightly with either the membrane and/or the lamina than the other nups examined. In an effort to differentiate between these possibilities, we first extracted NEs with the nonionic detergent Triton X-100. This treatment releases most NE membrane proteins with the exception of those that are tightly associated with the pelletable fraction containing NPCs attached to the lamina (Schirmer *et al.*, 2003). To compare the extractability of various nups from

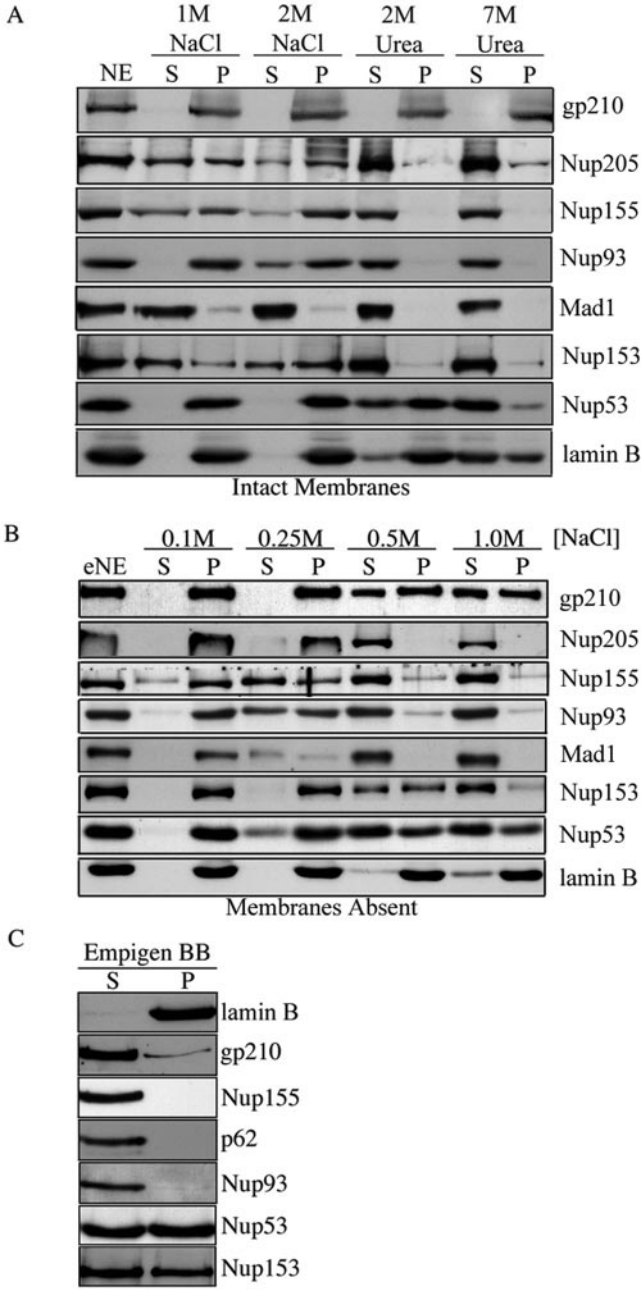

Figure 2. Nup53 interacts tightly with the nuclear envelope membrane and lamina. (A) Purified rat liver NEs were extracted with 1 M NaCl, 2 M NaCl, 2 M urea, or 7 M urea and then centrifuged to produce a supernatant fraction (S) and a membrane pellet (P) fraction. After separation of proteins by SDS-PAGE, fractions were analyzed by Western blotting using antibodies that bind the indicated proteins. (B) Alternatively, NE membranes were extracted with Triton X-100, and an insoluble NPC and lamina-containing fraction was recovered by centrifugation. This extracted NE (eNE) fraction was then treated with increasing concentrations of NaCl to release nups from the lamina. After centrifugation to produce supernatant and pellet fractions, proteins were analyzed by Western blotting as in A. (C) A previously described extraction protocol of NEs (Matunis *et al.*, 1996; Cronshaw *et al.*, 2002) that concludes with empigen BB-induced release of NPCs from the lamina was also used to evaluate the association of Nup53 with the lamina. After extraction with empigen BB and centrifugation, proteins in a nup-enriched (S) fraction and a lamin-enriched (P) fraction were analysis by Western blotting using the antibodies specific to the indicated proteins.

the lamina, the pellet fraction was then extracted with increasing concentrations of NaCl. As shown in Figure 2B, Nup93 and Nup155 are efficiently extracted from the lamina by 0.5 M NaCl, whereas Nup53, as well as Nup153, were more resistant to extraction with ~50% of each being extracted at similar concentrations of NaCl. These observations are consistent with previously proposed interactions between Nup153 and the lamina (Smythe *et al.*, 2000).

A differential extraction of Nup53 and Nup153 from the nuclear lamina was also observed when NEs were sequentially extracted with a Triton X-100/SDS cocktail followed by the zwitterionic detergent Empigen BB. Matunis and coworkers have previously shown that this procedure releases the nups into a soluble supernatant fraction and produces a pellet fraction consisting largely of lamins (Matunis *et al.*, 1996; Cronshaw *et al.*, 2002). However, Western blotting of these fractions showed that ~50% of Nup53 and Nup153 remained associated with the lamina fraction after Empigen BB extraction (Figure 2C). These represented a significantly higher level of retention with the lamina than observed with gp210, p62, and Nup155 (Figure 2C) and is higher than previously reported for most nups (Fontoura *et al.*, 1999; Cronshaw *et al.*, 2002). These results further support the idea that Nup53, like Nup153, is physically linked to the nuclear lamina.

Nup53 Interacts with Nup93, Nup155, and Nup205

We further investigated the physical interactions between Nup53 and neighboring proteins in the NE by attempting to reconstitute these interactions in vitro. For these experiments, rat liver NEs were treated with a combination of 1% Triton X-100 and 400 mM NaCl. These extraction conditions solubilized the nups and a significant fraction of the lamins (unpublished data). After dilution, the extract was incubated with a purified, recombinant GST-Nup53 fusion protein immobilized on glutathione Sepharose beads. NE proteins that bound GST-Nup53 were detected using SDS-PAGE and silver staining. Two prominent species of ~90 and 200 kDa (Figure 3A) were identified. Mass spectrometry analysis of peptide fragments derived from these polypeptides revealed that the 200 and 90 kDa proteins were Nup205 and Nup93, respectively (unpublished data), two nups that had previously been shown to interact with each other (Grandi *et al.*, 1997). These results were confirmed by Western blotting using Nup205 and Nup93 antibodies, which recognized the corresponding bands (Figure 3A). In an effort to identify any other Nup53-interacting partners, we also probed the eluted fraction with a variety of other antibodies. Interestingly, Western blotting using antibodies specific to Nup155 and lamin B detected both proteins in the GST-Nup53–bound fraction (Figure 3A). In contrast, we failed to detect a variety of other nups, including those nups recognized by mAb414 (Figure 3A), Nup107, Nup133, Nup160, and gp210 (unpublished data), as well as the NPC associated protein Mad1 (see below). Moreover, lamins A and C were generally not detected in bound fractions (Figure 3A).

In an effort to begin to map the interactions between Nup53 and the nups detected in the GST pulldown assay, we tested whether purified recombinant GST-Nup53 could bind directly to recombinant Nup93. When purified Nup93 was incubated with GST-Nup53 immobilized on glutathione Sepharose beads, it was largely retained in the bound fraction as detected by Coomassie blue staining and Western blotting with anti-Nup93 antibodies (Figure 3B). In contrast, no binding of Nup93 was detected to GST alone. This result suggests a direct interaction between Nup53 and Nup93.

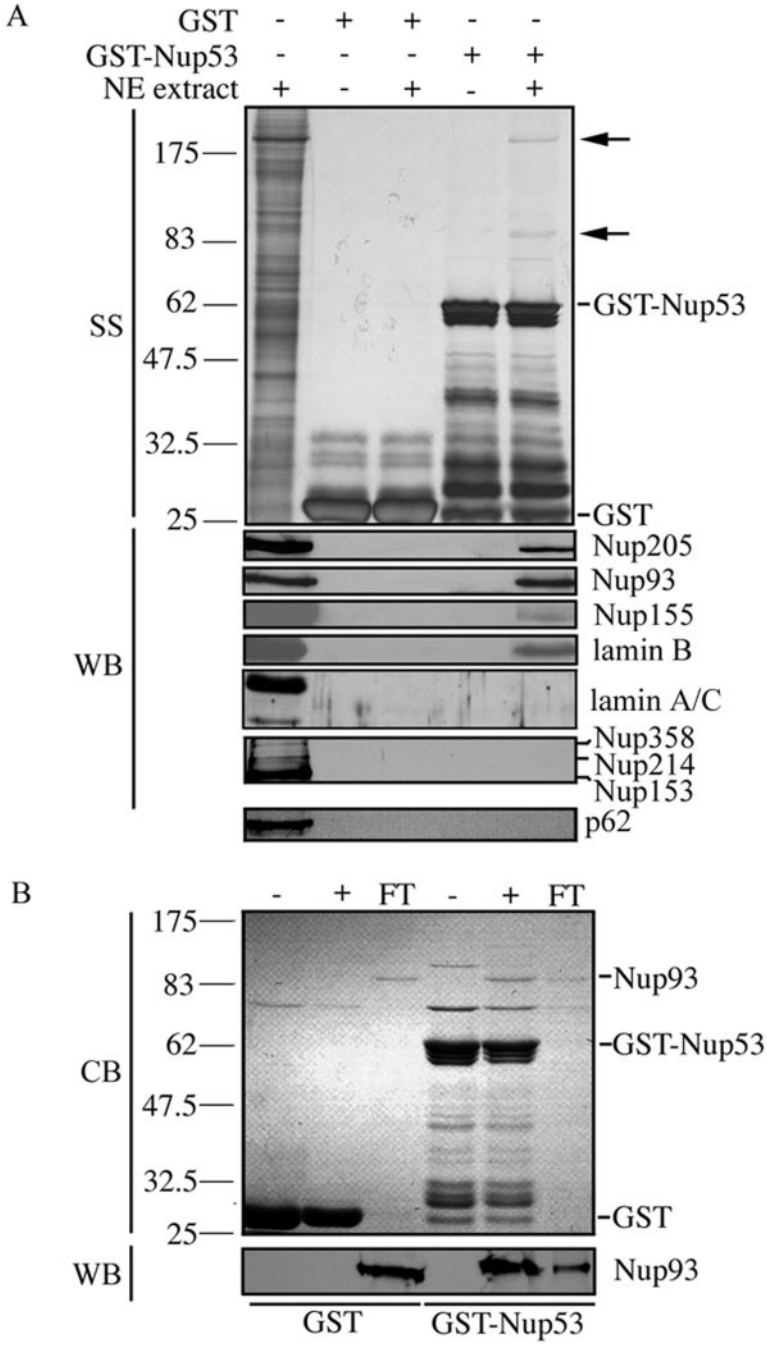

Figure 3. Identification of Nup53-interacting partners using in vitro binding assays. (A) Purified rat liver NEs were extracted with 400 mM NaCl and 1% Triton X-100. After centrifugation to remove insoluble material, the supernatant fraction, containing nups and lamins, was diluted 3.75-fold (NE extract) and incubated with purified recombinant GST-Nup53 or GST alone immobilized on glutathione Sepharose 4B beads. After binding and washing steps, the bead-bound proteins were eluted, separated by SDS-PAGE, and detected with silver staining (SS). Several representative protein species that specifically bound Nup53 are indicated with an arrow. Samples were also analyzed by Western blotting (WB) using polyclonal antibodies directed against the indicated proteins or mAb414 to detect Nup358, Nup214, Nup153, and p62. (B) Purified recombinant Nup93 was incubated with GST-Nup53 or GST alone immobilized on glutathione Sepharose 4B beads. After washing, beads were eluted with sample buffer. Proteins were separated by SDS-PAGE and analyzed by Coomassie Blue staining (CB) or Western blotting (WB) using antibodies directed against Nup93. The positions of mass markers in kilodaltons are indicated.

Depletion of Nup53 Inhibits the Assembly of Interacting nups and the Spindle Checkpoint Protein Mad1 into the NPC

In an effort to investigate cellular functions of Nup53, small interfering RNAs (siRNAs) specific for Nup53 mRNA were transfected into HeLa cells to deplete cellular levels of Nup53. After transfection, we monitored changes in both the level of mRNA and protein using RT-PCR and Western blotting, respectively. HeLa cells were transfected either with transfection reagent alone, nonsense siRNAs, or with human Nup53-specific siRNA duplexes. Levels of Nup53 mRNA were significantly reduced 48 h after transfection, whereas the level of mRNA encoding another nup, Nup155, was not affected, demonstrating the specificity of this approach (unpublished data). The reduced level of Nup53 mRNA was accompanied by a depletion of Nup53 as detected by Western blotting (Figure 4A). Consistent with these observations, immunofluorescence analysis revealed that levels of Nup53 at the NE were greatly reduced in 50–70% of the Nup53 siRNA-treated cells, whereas cells treated with nonsense siRNAs showed no change in the punctate nuclear rim staining (Figure 4B).

The siRNA-mediated depletion of Nup53 was accompanied by distinct changes in cell growth. As shown in Figure 5A, cell cultures treated with Nup53-specific siRNAs doubled at a rate approximately half that observed in cultures

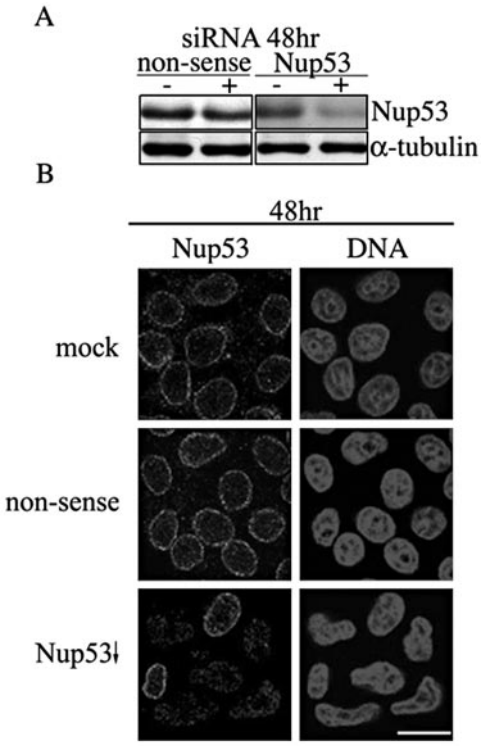

Figure 4. In vivo depletion of Nup53 using small interfering RNAs. (A) HeLa cells were incubated for 48 h in the presence of either transfection reagent alone (−) or siRNA (+) corresponding to nonsense siRNAs or Nup53 siRNAs. Samples were then collected and the cellular levels of Nup53 and α-tubulin (for comparison of total protein loaded in each fraction) were analyzed by Western blotting of total cell extracts. (B) HeLa cells growing on coverslips were incubated for 48 h with transfection reagent alone (mock), nonsense siRNAs (nonsense), or Nup53 (Nup53) siRNAs and processed for immunofluorescence. Cells were probed with anti-Nup53 antibodies, and binding was detected with Cy3-labeled secondary antibodies. Nuclear DNA was detected by staining with the DNA-binding dye Hoechst. Bar, 10 μm.

treated with nonsense siRNAs. The decreased growth rate observed was not due to changes in cell viability (unpublished data). Moreover, several assays suggested that the Nup53-depleted cells exhibited a general growth inhibition as they were not delayed in progression through a specific phase of the cell cycle. FACS analysis of both Nup53-depleted and nondepleted cells revealed similar profiles (Figure 5B). In addition, the number of cells in S-phase (as detected using bromodeoxyuridine labeling) and M-phase (as detected by Hoechst staining) were similar, ~40 and ~4%, respectively, in depleted and nondepleted cultures (unpublished data).

We next examined the effects of removing Nup53 on the assembly and stability of other nups in the NPC. At 48 h after Nup53 siRNA transfection, depleted cells were analyzed by immunofluorescence using antibodies directed against several nups including Nup93, Nup107, and the mAb414 reactive nups (p62, Nup214, Nup153, and Nup358). Levels of Nup107 and the mAb414 reactive nups were not affected by depletion of Nup53; however, we observed a striking decrease in the NE levels of Nup93 (Figure 6A). The loss of NE bound Nup93 was accompanied by a corresponding decrease in cellular levels of Nup93 as determined by Western blot analysis of whole cells extracts (Figure 6B). Similarly, we observed that other Nup53 interacting proteins (see above), including Nup155 and Nup205, were also present in reduced amounts in Nup53-depleted cells (Figure 6, A and B).

The Nup53 depletion data are consistent with the idea that Nup53, Nup93, Nup205, and Nup155 interact with one another and that Nup53 is required for the assembly and/or stability of these nups within the NPC. As a complement to these studies, we also examined the effects of depleting Nup93 on levels of other members of this interacting group. As shown in Figure 7, treatment of HeLa cells with Nup93-specific siRNAs reduced cellular levels of Nup93 and, as previously shown, the mAb414-reactive nups (Figure 7, A and B; Krull *et al.*, 2004). Similarly, depleting Nup93 reduced cellular levels of Nup53, Nup155, and Nup205, but did not affect levels of Nup107, gp210, Mad1, or lamin B (Figure 7). We have also performed in vitro binding experiments with GST-Nup93 and NE extracts similar to those described above using GST-Nup53 (Figure 3). As shown in Figure 7C, GST-Nup93 is capable of binding Nup53, Nup155, and Nup205, but not Nup107.

In yeast, physical and genetic interactions have also been detected between Nup53p and the spindle checkpoint protein Mad1p (Iouk *et al.*, 2002). Similarly, Mad1 is bound to the vertebrate NPC during interphase (Campbell *et al.*, 2001). We investigated the possible functional link between human Nup53 and Mad1 by examining the effects of siRNA induced Nup53 depletion on the localization and cellular levels of Mad1. As shown in Figure 6A, depletion of Nup53 was accompanied by decreased, but detectable, levels of Mad1 at the NPC as seen by immunofluorescence microscopy. Moreover, Western blot analysis showed that cellular levels of Mad1 were also decreased (Figure 6B). In contrast, depletion of Nup93 had no effect on Mad1 levels (see Figure 7, A and B).

Despite the reduced levels of Mad1 in the Nup53 depleted cells, we did not detect a clear defect in the spindle assembly checkpoint as judged by monitoring their ability to arrest in mitosis after treatment with microtubule destabilizing drugs (unpublished data). These results suggest sufficient Mad1 remains in the depleted cells to maintain an active checkpoint response.

Depletion of Nup53 or Nup93 Leads to Aberrant Nuclear Morphology

Strikingly, cells that were depleted of Nup53 or Nup93 exhibited an aberrant nuclear morphology that was not observed in mock-treated or nonsense siRNA-transfected cells (see Figures 4B, 6A, and 7B). Nuclei of the depleted cells uniformly lost their round or oval shape, and often appeared elongated, lobular, or kidney-shaped. Their shape directly reflected the shape of the chromatin mass, as the NE membrane appeared to maintain direct contact with its surface (see Figure 6A). To investigate the functional basis for this morphological defect, we looked at the patterns of various nuclear markers in nonsense siRNA transfected and the Nup53- or Nup93-depleted cells. In light of the data presented above suggesting that Nup53 interacts with nuclear lamins (Figures 2 and 3A), we examined lamin B and lamins A/C distribution in HeLa cells that had been treated for 48 h with Nup53 siRNAs. We observed that the levels of lamin B, lamins A/C, and the inner nuclear membrane protein emerin appeared to remain unchanged in these cells (see Figure 6A). Similarly, the localization of lamin B was not affected in cells depleted of Nup93.

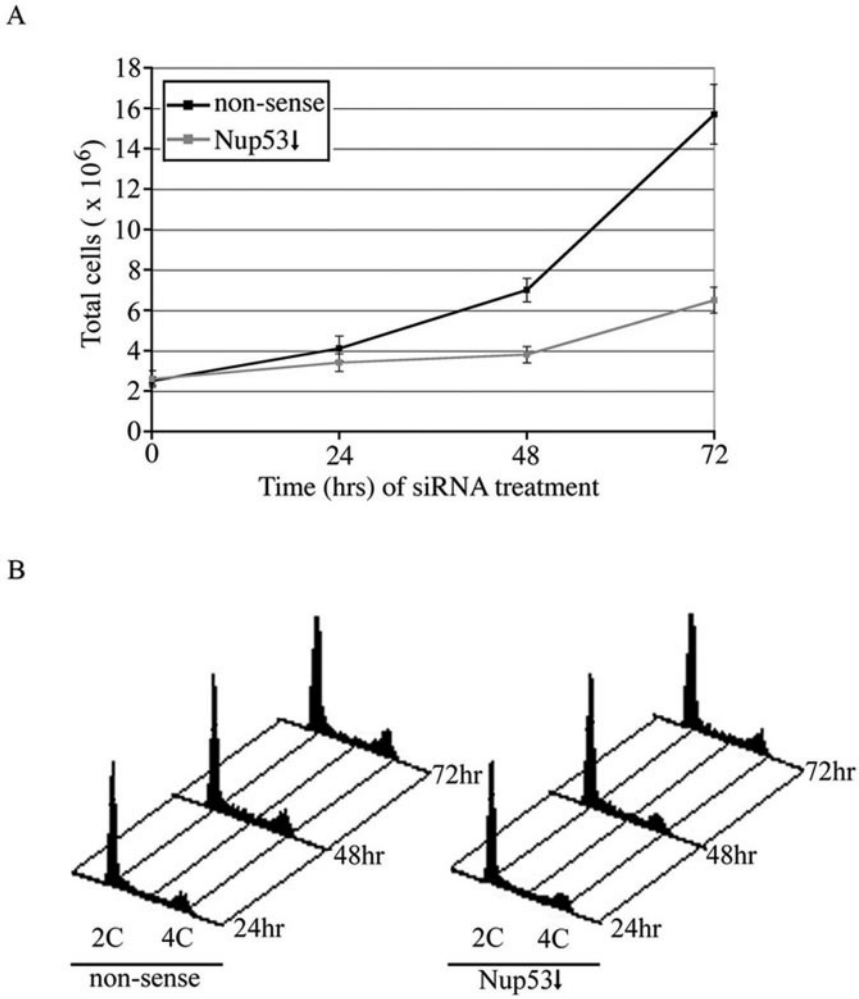

Figure 5. HeLa cells depleted of Nup53 exhibit a growth delay. (A) Equal numbers of HeLa cells were transfected with either nonsense or Nup53-specific siRNA duplexes and incubated for the indicated times. At each time point, cells were collected, their viability was assessed using trypan blue and the number of viable cells was plotted versus time. Note, both nonsense and Nup53-specific siRNA treated cells showed a similar viability (>90%). The results shown are representative of three separate trials. (B) As in A, HeLa cells were transfected with either nonsense or Nup53-specific siRNA duplexes and incubated for the indicated times. Cells were then collected and processed for FACS analysis. The positions of the 2C and 4C peaks are indicated.

DISCUSSION

Both morphological analysis and an accumulating body of biochemical data suggest that the NPC is composed of modular subunits consisting of specific subsets of nups. Several of these subcomplexes have been identified as a consequence of their resistance to extraction conditions that partially disassemble NPCs, whereas in other cases the functional complexes are inferred based on networks of interactions, both biochemical and genetic, detected between groups of nups. The conservation of the structural features of the NPC between different species suggests that the compositions of the subcomplexes are also conserved. However, sequence similarity between nups of yeast and vertebrates is variable and several nups present in one species have no clear counterparts in the other (see Cronshaw *et al.,* 2002). Thus, it remains to be determined to what degree individual subcomplexes are conserved.

Genetic and biochemical analyses have established that yeast Nup53p is part of a network of interacting nups that includes Nup170p, Nup59p, Nic96p, Nup157p, and Nup192p (Aitchison *et al.,* 1995b; Marelli *et al.,* 1998; Kosova *et al.,* 1999; Fahrenkrog *et al.,* 2000; Lusk *et al.,* 2002; Makhnevych *et al.,* 2003). A model for how these nups are organized within the NPC is beginning to emerge. Nup53p can bind directly to Nup170p and Nic96p (Lusk *et al.,* 2002; Makhnevych *et al.,* 2003; Lusk and Wozniak, unpublished data). However, their interactions are cell cycle regulated. Nup53p binds to Nup170p during interphase, which blocks the ability of Nup53p to bind the karyopherin Kap121p. In contrast, during mitosis Nup53p is no longer detected in association with Nup170p but is instead bound to Nic96p and Kap121p (Makhnevych *et al.,* 2003). How Nup59p, Nup157p, and Nup192p fit into this developing model is less clear. Proposals must consider the fact that Nup59p and Nup157p are likely products of gene duplications that also gave rise to Nup53p and Nup170p, respectively (Aitchison *et al.,* 1995b; Marelli *et al.,* 1998). Thus, although these pairs of related proteins are not functionally identical, it is possible that they are structurally interchangeable within the repetitive subunits of the NPC, creating a mosaic of structurally similar subcomplexes composed of different combinations of these related nups. In contrast to the redundancy observed in yeast, vertebrate Nup53 and Nup155 (the ortholog of Nup170p and Nup157p) represent the only forms of these nups. Together with Nup93 (the ortholog of yeast Nic96p) and Nup205 (the ortholog of yeast Nup192p) they likely form a similar, evolutionarily conserved, structure. We interpret the lack of paralogs in vertebrates to suggest that these Nup53-containing complexes are more homogenous and potentially lack certain functions that have evolved in the yeast counterpart (see Makhnevych *et al.,* 2003). This may include the ability to regulate import con-

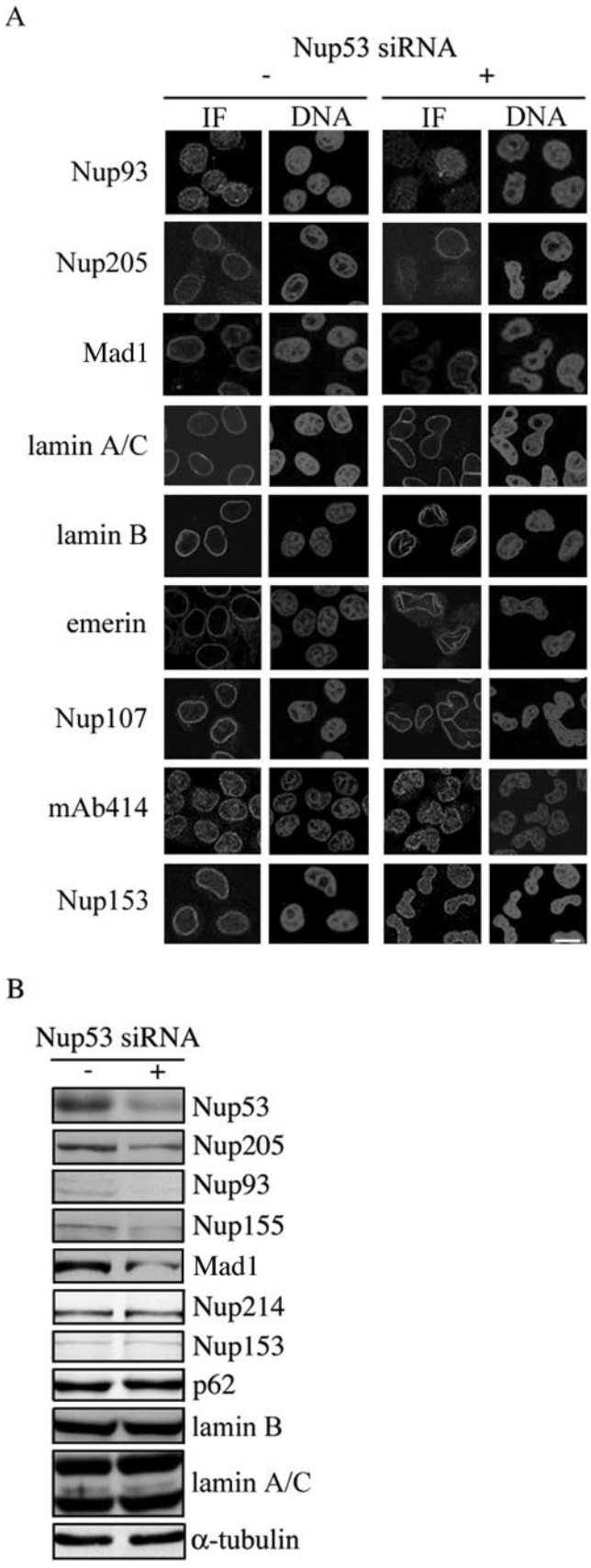

trolled by the mammalian counterpart of Kap121p, because vertebrate Nup53 lacks the Kap121p-binding domain found in yeast Nup53p.

On the basis of data presented in this article and by analogy to the yeast NPC, we propose that Nup53 interacts with Nup155 and a previously identified Nup93-Nup205 complex (Grandi *et al.*, 1997). This latter complex may also be physically associated with Nup188 (Miller *et al.*, 2000), the yeast ortholog of which has been functionally linked to Nup53p and Nup170p (Aitchison *et al.*, 1995b; Marelli *et al.*, 1998). We have shown that both GST-Nup53 and GST-Nup93 are capable of binding Nup155 and Nup205, as well as Nup93 and Nup53, respectively. These data and the observed decreases in cellular levels of these nups in response to depletion of either Nup53 or Nup93 suggest they exist as a complex within the NPC. This complex, however, has been refractory to direct isolation, likely because it is labile under conditions required to disassemble the NPC. For example, extraction conditions that have allowed the identification of complexes containing Nup107-Nup133 or gp210 on sucrose gradients appear to largely produce monomeric Nup53, Nup93, and Nup155 (see Supplementary Figure 1).

This group of nups likely contributes to the symmetrical core structures of the NPC. Recent immunoelectron microscopy data from Krull *et al.* (2004) suggest that both Nup93 and Nup205 are centrally positioned within the NPC near the pore membrane. Also consistent with this idea, Nup155 is symmetrically distributed on both faces of the NPC (Radu *et al.*, 1993). In addition, we observed that Nup53 is accessible to cytoplasmically presented antibodies in the presence or absence of the NE membrane (see Supplementary Figure 2). The localization of these nups to the NPC core is also consistent with data showing that Nup93 and Nup205 play a role in the permeability of the NPC (Galy *et al.*, 2003), a property that is shared with the yeast counterpart of Nup155 (Shulga *et al.*, 2000).

Data are also consistent with the idea that this complex of nups lies near the circumference of the NPC at the pore membrane. This conclusion is based both on the localization of Nup93 and Nup205 as discussed above (Krull *et al.*, 2004) and on the tight association between Nup53 and the NE membrane. We have shown, using various urea extraction conditions, that the release of Nup53 from the NE membrane appears to largely parallel that of the lamins, requiring significantly higher concentrations of urea for extraction from the membrane than other nups. These results are similar to those previously documented with yeast Nup53p (Marelli *et al.*, 2001). In yeast, the association of Nup53p with the membrane was shown to be dependent on a putative amphipathic helix at its C-terminus, a structure that also

Figure 6. In vivo depletion of Nup53 leads to codepletion of a subset of interacting nups and the mitotic checkpoint protein Mad1. (A) Forty-eight hours after the transfection of HeLa cells with either nonsense (−) or Nup53 (+) siRNAs, cells were processed for indirect immunofluorescence (IF). Samples were probed with antibodies directed against the indicated proteins, and binding was detected with Cy3-labeled secondary antibodies. Mab414 binding was detected with FITC-labeled secondary antibodies. Nuclear DNA was detected by staining with the DNA-binding dye Hoechst (DNA). Bar, 10 μm. (B) Cells were transfected as described in A, total cell extracts were isolated, and proteins were separated by SDS-PAGE. Western blot analysis was performed using antibodies directed against the indicated proteins. Note, mAb414 was used to visualize the levels of p62, Nup153, and Nup214. Antibodies directed against α-tubulin were used for comparing total protein loads in each fraction.

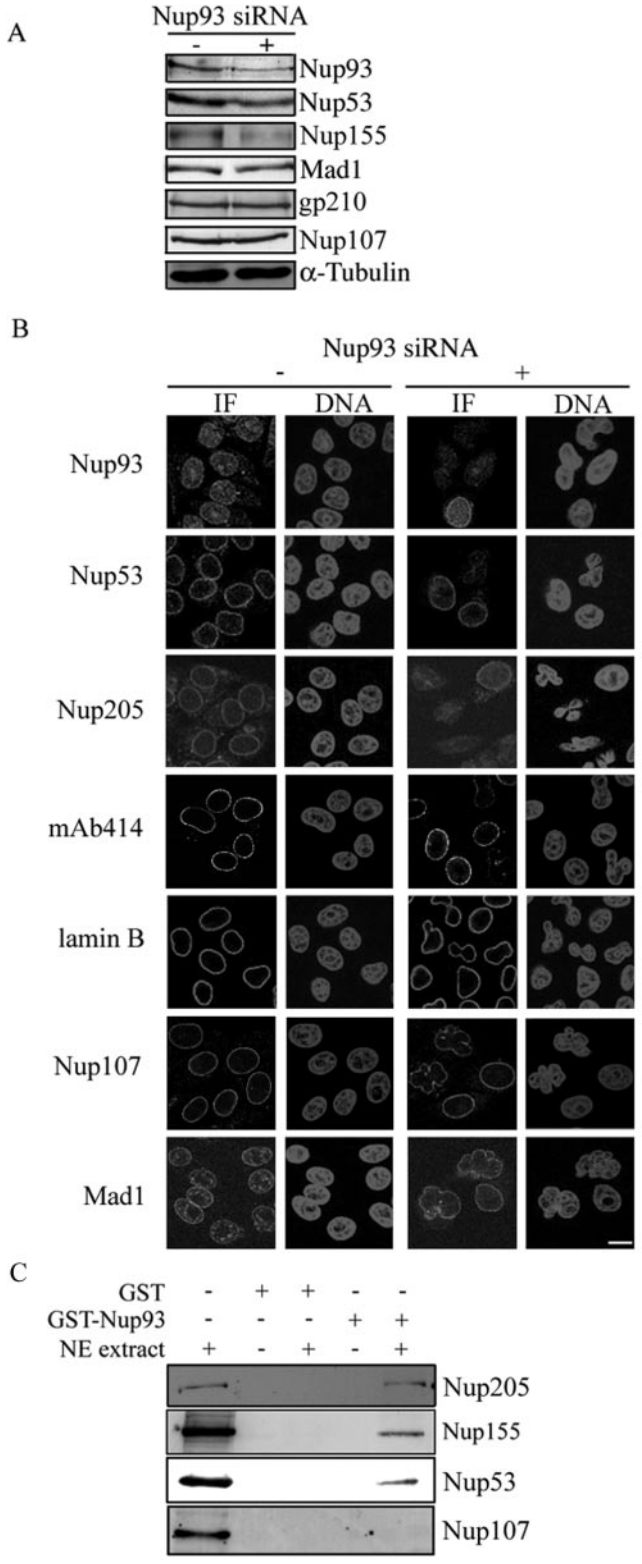

Figure 7. In vivo depletion of Nup93 and the identification Nup93-interacting partners using in vitro binding assays. (A) Forty-eight hours after the transfection of HeLa cells with either nonsense (−) or Nup93 (+) siRNAs, total cell extracts were isolated, and proteins were separated by SDS-PAGE. Western blot analysis was performed using antibodies directed against the indicated proteins. Antibodies directed against α-tubulin were used for comparing total protein loads in each fraction. (B) Cells were transfected as described in A and processed for indirect immunofluorescence (IF). Samples were probed with antibodies directed against the indicated proteins, and binding was detected with Cy3-labeled secondary antibodies. Mab414 binding was detected with FITC-labeled secondary antibodies. Nuclear DNA was detected by staining with the DNA-binding dye Hoechst (DNA). Bar, 10 μm. (C) Purified recombinant GST-Nup93 or GST alone were immobilized on glutathione Sepharose 4B and incubated with or without rat liver NE extracts as described for Nup53 in Figure 3A. The bead-bound proteins were eluted, separated by SDS-PAGE, and analyzed by Western blotting using antibodies directed against the indicated nups.

appears to be present within the last 13 amino acid residues of vertebrate Nup53. Nup53 also appears to interact with the nuclear lamina. We have observed that Nup53 remains tightly associated with the lamina after removal of the NE membrane with detergent (Figure 2B). Moreover, we have detected lamin B bound to recombinant Nup53 using in vitro binding assays (Figure 3A) and we have observed that Nup53 and lamin B cosediment on sucrose gradients (Supplementary Figure 1). In the aggregate, our data support a model in which Nup53 is positioned at the interface between the pore membrane and the lamina where it could anchor other nups to these structures.

Nup53 is one of two nups that have so far been implicated in linking the NPC to the nuclear lamina. Smythe *et al.* (2000) have suggested that *Xenopus* Nup153 binds to lamin B_3. Nup153 is located on the nuclear side of the NPC (Cordes *et al.*, 1993; Sukegawa and Blobel, 1993) and it has been suggested that it links the core structures to the nuclear basket and the nuclear filamentous protein Tpr (Krull *et al.*, 2004). These data place Nup153 in a separate subcomplex from the core associated Nup53. Considering these data and ours, its would seem possible that different subcomplexes of the NPC may possess distinct lamin binding members, with Nup53 functioning to link the Nup93-containing complex, and perhaps more generally the NPC core, to the nuclear lamina.

At the pore membrane Nup53 is strategically positioned to function in the assembly of nups into a forming NPC. Using RNA interference to deplete endogenous Nup53, we showed that reducing the cellular levels of Nup53 produced a corresponding decrease in Nup93, Nup205, and Nup155, while not affecting other nup complexes (Figure 6). A likely explanation for this phenomenon is that reduced levels of Nup53 inhibit the assembly of these nups into the NPC, leading to unstable, partially assembled complexes that are more rapidly degraded. Similar results have also been documented for other nup complexes, including the depletion of the Nup107-Nup160 complex, where the stability of the complex is decreased by depletion of individual members (Boehmer *et al.*, 2003; Harel *et al.*, 2003; Walther *et al.*, 2003).

A striking consequence of depleting Nup53 is the loss of normal nuclear morphology. Nup53-depleted cells lose their spherical shape, generally adopting an elongated lobular or kidney-shape. This observation was intriguing in light of the interactions between Nup53 and the lamina and the similarity of this morphology to that previously detected in cells lacking lamin A (Sullivan *et al.*, 1999). However, we have not observed any interactions between Nup53 and lamin A/C nor have we detected changes in the levels or the distribution of the lamins or the inner membrane protein emerin (Figure 6). Both of these classes of proteins are evenly distributed along the irregular nuclear periphery of the Nup53-depleted cells, each following the contour of the underlying chromatin mass. Thus, the relationship between the nuclear morphologies of cells lacking Nup53 and the lamin A–de-

pleted cells is unclear. Not surprisingly, we also observed a similar phenotype in cells depleted of Nup93 where levels of Nup53 are also reduced. This raises the question of whether the altered nuclear morphology is related directly to the loss of Nup53 function or whether it is a result of the codepletion of Nup93 or other interacting nups.

Depletion analysis of the *C. elegans* counterparts of the Nup93, Nup205, Nup155, and Nup53, has also been performed in embryos. This study conducted by Galy *et al.* (2003) suggests that distinct morphological phenotypes are associated with the depletion of these nups. Although depletion of each causes an embryonic lethal phenotype, depletion of the counterparts of Nup53 or Nup155 appears to block nuclear formation after mitosis. The cause of this block is yet to be determined. In contrast, embryos lacking Nup93 and Nup205 exhibit abnormal peripheral chromatin condensation and what appears to be an altered distribution of NPCs in the NE. We have not detected similar phenotypes in HeLa cells depleted of either Nup53 or Nup93 (Figures 6A and 7B; unpublished data). Moreover, unlike the depleted HeLa cells, the *C. elegans* embryos lacking counterparts of Nup93 or Nup53 do not exhibit any alterations in nuclear shape (Galy *et al.*, 2003).

A disruption of nuclear morphology similar to that detected in cells depleted of Nup53 was also observed in cell lines depleted of Mad1 (Luo *et al.*, 2002). The most well-defined function of Mad1 is its role in the spindle assembly checkpoint, a quality control feature of chromosome segregation that monitors spindle attachment to kinetochores during mitosis (reviewed in Lew and Burke, 2003). Intriguingly, Mad1 is localized to the NPC during interphase in both mammalian and yeast cells (Campbell *et al.*, 2001; Iouk *et al.*, 2002). However, it remains to be determined what function the association of Mad1 with the NPC plays in the spindle assembly checkpoint or to what degree Mad1 contributes to the function of the NPC. In yeast, the docking of Mad1p to the NPC has been shown to occur, in part, through its interaction with the Nup53p-containing complex (Iouk *et al.*, 2002). Consistent with this, yeast cells exhibit diminished levels of Mad1p at the NPC in *nup53*Δ cells (Iouk *et al.*, 2002). Our data are consistent with a similar interaction occurring in mammalian cells, where the levels of Mad1 are reduced, but still detectable, at the NE in the Nup53-depleted cells (Figure 6). We conclude from these observations that Mad1 may interact with more than one nup at the NPC. Of note, siRNA induced depletion of Nup93, which reduces NE levels of Nup53, does not appear to alter cellular levels of Mad1. A potential explanation for these results is that Mad1 interacts with a separate pool of Nup53 distinct from that bound to the Nup93-containing complex.

Previous studies of cell lines specifically depleted of Mad1 using RNA interference have shown that these cells exhibit defects in spindle checkpoint function (Martin-Lluesma *et al.*, 2002). We have performed similar experiments on Nup53-depleted cells to determine whether the reduced NPC association and cellular levels of Mad1 are sufficient to abrogate spindle checkpoint function. However, we failed to detect an obvious chromosome segregation defect (unpublished data) that would suggest that this pathway is inhibited. Presumably, sufficient levels of Mad1 remain to conduct its essential role in spindle checkpoint function. What role the NPC association plays in the function of this remaining pool of Mad1 will await the identification of its other NPC binding sites.

During prometaphase Mad1 is recruited to kinetochores (Chen *et al.*, 1998; Campbell *et al.*, 2001). In contrast, we have not detected Nup53 (using either indirect immunofluorescence or GFP fusions) or Nup93 at kinetochores during mitosis, suggesting that any interaction of Mad1 with Nup53 is not maintained at the kinetochores. Of note, members of the Nup107-containing complex and Nup358 (RanBP2), although largely distributed throughout the cytoplasm during mitosis, have also been detected at kinetochores (Belgareh *et al.*, 2001; Joseph *et al.*, 2002; Loïodice *et al.*, 2004). The functional role of the Nup107-Nup160 complex at kinetochores is not established and no specific defects in the function of this structure have been attributed to the depletion of these nups. In contrast, depletion of Nup358 leads to severe defects in kinetochore structure and a reduction in the recruitment of Mad1 and Mad2 to kinetochores (Salina *et al.*, 2003; Joseph *et al.*, 2004). However, the spindle checkpoint remains active in these cells. Thus it appears unlikely that these nups play a critical role in basal levels of spindle checkpoint activity. A more plausible scenario is that the association of nups with kinetochores, as well as interactions of the Mads with the NPC, may function to regulate the fidelity of the spindle checkpoint response.

ACKNOWLEDGMENTS

Protein identification was performed at the Institute for Biomolecular Design, University of Alberta. We thank John Aitchison and members of the Wozniak laboratory for helpful discussions and Andrew Chau for technical assistance in the production of GST-xNup53. We are also grateful to those cited in the text for their generous gifts of antibodies. We also thank Honey Chan for help with confocal microscopy. Nup93 cDNA was obtained from Dr. Takahiro Nagase at the Kazusa DNA Research Institute, Japan. Funding for this work was provided by the Canadian Institutes for Health Research and the Alberta Heritage Foundation for Medical Research.

REFERENCES

Aitchison, J. D., Blobel, G., and Rout, M. P. (1995a). Nup120p: a yeast nucleoporin required for NPC distribution and mRNA transport. J. Cell Biol. *131*, 1659–1675.

Aitchison, J. D., Rout, M. P., Marelli, M., Blobel, G., and Wozniak, R.W. (1995b). Two novel related yeast nucleoporins Nup170p and Nup157p: complementation with the vertebrate homologue Nup155p and functional interactions with the yeast nuclear pore-membrane protein Pom152p. J. Cell Biol. *131*, 1133–1148.

Allen, N. P., Patel, S. S., Huang, L., Chalkley, R. J., Burlingame, A., Lutzmann, M., Hurt, E. C., and Rexach, M. (2002). Deciphering networks of protein interactions at the nuclear pore complex. Mol. Cell Proteomics *1*, 930–946.

Belgareh, N., and Doye, V. (1997). Dynamics of nuclear pore distribution in nucleoporin mutant yeast cells. J. Cell Biol. *136*, 747–759.

Belgareh, N. *et al.* (2001). An evolutionarily conserved NPC subcomplex, which redistributes in part to kinetochores in mammalian cells. J. Cell Biol. *154*, 1147–1160.

Blobel, G., and Potter, V. R. (1966). Nuclei from rat liver: isolation method that combines purity with high yield. Science *154*, 1662–1665.

Boehmer, T., Enninga, J., Dales, S., Blobel, G., and Zhong, H. (2003). Depletion of a single nucleoporin, Nup107, prevents the assembly of a subset of nucleoporins into the nuclear pore complex. Proc. Natl. Acad. Sci. USA *100*, 981–985.

Burke, B. (2001). Lamins and apoptosis: a two-way street? J. Cell Biol. *153*, F5–F7.

Campbell, M. S., Chan, G. K., and Yen, T. J. (2001). Mitotic checkpoint proteins HsMAD1 and HsMAD2 are associated with nuclear pore complexes in interphase. J. Cell Sci. *114*, 953–963.

Chaudhary, N., and Courvalin, J. C. (1993). Stepwise reassembly of the nuclear envelope at the end of mitosis. J. Cell Biol. *122*, 295–306.

Chen, R. H., Shevchenko, A., Mann, M., and Murray, A. W. (1998). Spindle checkpoint protein Xmad1 recruits Xmad2 to unattached kinetochores. J. Cell Biol. *143*, 283–295.

Cordes, V. C., Reidenbach, S., Kohler, A., Stuurman, N., van Driel, R., and Franke, W. W. (1993). Intranuclear filaments containing a nuclear pore complex protein. J. Cell Biol. *123*, 1333–1344.

Cronshaw, J. M., Krutchinsky, A. N., Zhang, W., Chait, B. T., and Matunis, M. J. (2002). Proteomic analysis of the mammalian nuclear pore complex. J. Cell Biol. *158*, 915–927.

De Souza, C. P., Horn, K. P., Masker, K., and Osmani, S. A. (2003). The SONB(NUP98) nucleoporin interacts with the NIMA kinase in *Aspergillus nidulans.* Genetics *165*, 1071–1081.

De Souza, C. P., Osmani, A. H., Hashmi, S. B., and Osmani, S. A. (2004). Partial nuclear pore complex disassembly during closed mitosis in *Aspergillus nidulans.* Curr. Biol. *14*, 1973–1984.

Elbashir, S. M., Harborth, J., Lendeckel, W., Yalcin, A., Weber, K., and Tuschl, T. (2001). Duplexes of 21-nucleotide RNAs mediate RNA interference in cultured mammalian cells. Nature *411*, 494–498.

Fahrenkrog, B., Hubner, W., Mandinova, A., Pante, N., Keller, W., and Aebi, U. (2000). The yeast nucleoporin Nup53p specifically interacts with Nic96p and is directly involved in nuclear protein import. Mol. Biol. Cell *11*, 3885–3896.

Fontoura, B. M., Blobel, G., and Matunis, M. J. (1999). A conserved biogenesis pathway for nucleoporins: proteolytic processing of a 186-kilodalton precursor generates Nup98 and the novel nucleoporin, Nup96. J. Cell Biol. *144*, 1097–1112.

Galy, V., Mattaj, I. W., and Askjaer, P. (2003). *Caenorhabditis elegans* nucleoporins Nup93 and Nup205 determine the limit of nuclear pore complex size exclusion in vivo. Mol. Biol. Cell *14*, 5104–5115.

Gilchrist, D., Mykytka, B., and Rexach, M. (2002). Accelerating the rate of disassembly of karyopherin.cargo complexes. J. Biol. Chem. *277*, 18161–18172.

Grandi, P., Dang, T., Pane, N., Shevchenko, A., Mann, M., Forbes, D., and Hurt, E. (1997). Nup93, a vertebrate homologue of yeast Nic96p, forms a complex with a novel 205-kDa protein and is required for correct nuclear pore assembly. Mol. Biol. Cell *8*, 2017–2038.

Grandi, P., Schlaich, N., Tekotte, H., and Hurt, E. C. (1995). Functional interaction of Nic96p with a core nucleoporin complex consisting of Nsp1p, Nup49p and a novel protein Nup57p. EMBO J. *14*, 76–87.

Harborth, J., Elbashir, S. M., Bechert, K., Tuschl, T., and Weber, K. (2001). Identification of essential genes in cultured mammalian cells using small interfering RNAs. J. Cell Sci. *114*, 4557–4565.

Harel, A., Orjalo, A. V., Vincent, T., Lachish-Zalait, A., Vasu, S., Shah, S., Zimmerman, E., Elbaum, M., and Forbes, D. J. (2003). Removal of a single pore subcomplex results in vertebrate nuclei devoid of nuclear pores. Mol. Cell *11*, 853–864.

Harlow, F., and Lane, D. (1988). Antibodies: A Laboratory Manual, Cold Spring Harbor, NY: Cold Spring Harbor Laboratory.

Iouk, T., Kerscher, O., Scott, R. J., Basrai, M. A., and Wozniak, R. W. (2002). The yeast nuclear pore complex functionally interacts with components of the spindle assembly checkpoint. J. Cell Biol. *159*, 807–819.

Joseph, J., Liu, S. T., Jablonski, S. A., Yen, T. J., and Dasso, M. (2004). The RanGAP1-RanBP2 complex is essential for microtubule-kinetochore interactions in vivo. Curr. Biol. *14*, 611–617.

Joseph, J., Tan, S. H., Karpova, T. S., McNally, J. G., and Dasso, M. (2002). SUMO-1 targets RanGAP1 to kinetochores and mitotic spindles. J. Cell Biol. *156*, 595–602.

Kosova, B., Pante, N., Rollenhagen, C., and Hurt, E. (1999). Nup192p is a conserved nucleoporin with a preferential location at the inner site of the nuclear membrane. J. Biol. Chem. *274*, 22646–22651.

Krull, S., Thyberg, J., Bjorkroth, B., Rackwitz, H. R., and Cordes, V. C. (2004). Nucleoporins as components of the nuclear pore complex core structure and tpr as the architectural element of the nuclear basket. Mol. Biol. Cell *15*, 4261–4277.

Lew, D. J., and Burke, D. J. (2003). The spindle assembly and spindle position checkpoints. Annu. Rev. Genet. *37*, 251–282.

Loïodice, I., Alves, A., Rabut, G., Van Overbeek, M., Ellenberg, J., Sibarita, J. B., and Doye, V. (2004). The entire Nup107–160 complex, including three new members, is targeted as one entity to kinetochores in mitosis. Mol. Biol. Cell *15*, 3333–3344.

Luo, X., Tang, Z., Rizo, J., and Yu, H. (2002). The Mad2 spindle checkpoint protein undergoes similar major conformational changes upon binding to either Mad1 or Cdc20. Mol. Cell *9*, 59–71.

Lusk, C. P., Makhnevych, T., Marelli, M., Aitchison, J. D., and Wozniak, R. W. (2002). Karyopherins in nuclear pore biogenesis: a role for Kap121p in the assembly of Nup53p into nuclear pore complexes. J. Cell Biol. *159*, 267–278.

Lutzmann, M., Kunze, R., Buerer, A., Aebi, U., and Hurt, E. (2002). Modular self-assembly of a Y-shaped multiprotein complex from seven nucleoporins. EMBO J. *21*, 387–397.

Macara, I. G. (2001). Transport into and out of the nucleus. Microbiol. Mol. Biol. Rev. *65*, 570–594, table of contents.

Makhnevych, T., Lusk, C. P., Anderson, A. M., Aitchison, J. D., and Wozniak, R. W. (2003). Cell cycle regulated transport controlled by alterations in the nuclear pore complex. Cell *115*, 813–823.

Marelli, M., Aitchison, J. D., and Wozniak, R. W. (1998). Specific binding of the karyopherin Kap121p to a subunit of the nuclear pore complex containing Nup53p, Nup59p, and Nup170p. J. Cell Biol. *143*, 1813–1830.

Marelli, M., Lusk, C. P., Chan, H., Aitchison, J. D., and Wozniak, R. W. (2001). A link between the synthesis of nucleoporins and the biogenesis of the nuclear envelope. J. Cell Biol. *153*, 709–724.

Martin-Lluesma, S., Stucke, V. M., and Nigg, E. A. (2002). Role of Hec1 in spindle checkpoint signaling and kinetochore recruitment of Mad1/Mad2. Science *297*, 2267–2270.

Mattaj, I. W. (2004). Sorting out the nuclear envelope from the endoplasmic reticulum. Nat. Rev. Mol. Cell. Biol. *5*, 65–69.

Mattout-Drubezki, A., and Gruenbaum, Y. (2003). Dynamic interactions of nuclear lamina proteins with chromatin and transcriptional machinery. Cell Mol. Life Sci. *60*, 2053–2063.

Matunis, M. J., Coutavas, E., and Blobel, G. (1996). A novel ubiquitin-like modification modulates the partitioning of the Ran-GTPase-activating protein RanGAP1 between the cytosol and the nuclear pore complex. J. Cell Biol. *135*, 1457–1470.

Miller, B. R., Powers, M., Park, M., Fischer, W., and Forbes, D. J. (2000). Identification of a new vertebrate nucleoporin, Nup188, with the use of a novel organelle trap assay. Mol. Biol. Cell *11*, 3381–3396.

Nehrbass, U., Rout, M. P., Maguire, S., Blobel, G., and Wozniak, R. W. (1996). The yeast nucleoporin Nup188p interacts genetically and physically with the core structures of the nuclear pore complex. J. Cell Biol. *133*, 1153–1162.

Radu, A., Blobel, G., and Wozniak, R. W. (1993). Nup155 is a novel nuclear pore complex protein that contains neither repetitive sequence motifs nor reacts with WGA. J. Cell Biol. *121*, 1–9.

Ribbeck, K., and Gorlich, D. (2001). Kinetic analysis of translocation through nuclear pore complexes. EMBO J. *20*, 1320–1330.

Ribbeck, K., and Gorlich, D. (2002). The permeability barrier of nuclear pore complexes appears to operate via hydrophobic exclusion. EMBO J. *21*, 2664–2671.

Rout, M. P., Aitchison, J. D., Magnasco, M. O., and Chait, B. T. (2003). Virtual gating and nuclear transport: the hole picture. Trends Cell Biol. *13*, 622–628.

Rout, M. P., Aitchison, J. D., Suprapto, A., Hjertaas, K., Zhao, Y., and Chait, B. T. (2000). The yeast nuclear pore complex: composition, architecture, and transport mechanism. J. Cell Biol. *148*, 635–651.

Ryan, K. J., and Wente, S. R. (2000). The nuclear pore complex: a protein machine bridging the nucleus and cytoplasm. Curr. Opin. Cell Biol. *12*, 361–371.

Salina, D., Enarson, P., Rattner, J. B., and Burke, B. (2003). Nup358 integrates nuclear envelope breakdown with kinetochore assembly. J. Cell Biol. *162*, 991–1001.

Schirmer, E. C., Florens, L., Guan, T., Yates, J. R., 3rd, and Gerace, L. (2003). Nuclear membrane proteins with potential disease links found by subtractive proteomics. Science *301*, 1380–1382.

Shulga, N., Mosammaparast, N., Wozniak, R., and Goldfarb, D. S. (2000). Yeast nucleoporins involved in passive nuclear envelope permeability. J. Cell Biol. *149*, 1027–1038.

Siniossoglou, S., Lutzmann, M., Santos-Rosa, H., Leonard, K., Mueller, S., Aebi, U., and Hurt, E. (2000). Structure and assembly of the Nup84p complex. J. Cell Biol. *149*, 41–54.

Siniossoglou, S., Wimmer, C., Rieger, M., Doye, V., Tekotte, H., Weise, C., Emig, S., Segref, A., and Hurt, E. C. (1996). A novel complex of nucleoporins, which includes Sec13p and a Sec13p homolog, is essential for normal nuclear pores. Cell *84*, 265–275.

Smythe, C., Jenkins, H. E., and Hutchison, C. J. (2000). Incorporation of the nuclear pore basket protein nup153 into nuclear pore structures is dependent upon lamina assembly: evidence from cell-free extracts of *Xenopus* eggs. EMBO J. *19*, 3918–3931.

Sukegawa, J., and Blobel, G. (1993). A nuclear pore complex protein that contains zinc finger motifs, binds DNA, and faces the nucleoplasm. Cell *72*, 29–38.

Sullivan, T., Escalante-Alcalde, D., Bhatt, H., Anver, M., Bhat, N., Nagashima, K., Stewart, C. L., and Burke, B. (1999). Loss of A-type lamin expression compromises nuclear envelope integrity leading to muscular dystrophy. J. Cell Biol. *147*, 913–920.

Vasu, S., Shah, S., Orjalo, A., Park, M., Fischer, W. H., and Forbes, D. J. (2001). Novel vertebrate nucleoporins Nup133 and Nup160 play a role in mRNA export. J. Cell Biol. *155*, 339–354.

Walther, T. C. *et al.* (2003). The conserved Nup107–160 complex is critical for nuclear pore complex assembly. Cell *113*, 195–206.

Weis, K. (2003). Regulating access to the genome: nucleocytoplasmic transport throughout the cell cycle. Cell *112*, 441–451.

Wozniak, R. W., Bartnik, E., and Blobel, G. (1989). Primary structure analysis of an integral membrane glycoprotein of the nuclear pore. J. Cell Biol. *108*, 2083–2092.

Yang, Q., Rout, M. P., and Akey, C. W. (1998). Three-dimensional architecture of the isolated yeast nuclear pore complex: functional and evolutionary implications. Mol. Cell *1*, 223–234.

Yoshida, K., and Blobel, G. (2001). The karyopherin Kap142p/Msn5p mediates nuclear import and nuclear export of different cargo proteins. J. Cell Biol. *152*, 729–740.

Zabel, U., Doye, V., Tekotte, H., Wepf, R., Grandi, P., and Hurt, E. C. (1996). Nic96p is required for nuclear pore formation and functionally interacts with a novel nucleoporin, Nup188p. J. Cell Biol. *133*, 1141–1152.